

# Behavior of Ising Spin Glasses in a Magnetic Field

Thomas Jörg,<sup>1,2</sup> Helmut G. Katzgraber,<sup>3</sup> and Florent Krzakala<sup>4</sup>

<sup>1</sup>LPTMS, UMR 8626 CNRS et Université Paris-Sud, 91405 Orsay CEDEX, France

<sup>2</sup>Équipe TAO - INRIA Futurs, 91405 Orsay CEDEX, France

<sup>3</sup>Theoretische Physik, ETH Zürich, CH-8093 Zürich, Switzerland

<sup>4</sup>Laboratoire PCT, UMR Gulliver CNRS-ESPCI 7083, 10 rue Vauquelin, 75231 Paris, France

We study the existence of a spin-glass phase in a field using Monte Carlo simulations performed along a nontrivial path in the field–temperature plane that must cross any putative de Almeida-Thouless instability line. The method is first tested on the Ising spin glass on a Bethe lattice where the instability line separating the spin glass from the paramagnetic state is also computed analytically. While the instability line is reproduced by our simulations on the mean-field Bethe lattice, no such instability line can be found numerically for the short-range three-dimensional model.

PACS numbers: 75.50.Lk, 75.40.Mg, 05.50.+q, 64.60.-i

Since its proposal in the mid-70’s, the Edwards and Anderson Ising spin-glass Hamiltonian has become a source of inspiration in statistical physics, especially in the context of mean field theory [1, 2, 3, 4], and has been applied to a wide variety of problems across scientific disciplines. However, basic yet simple questions about the very nature of the spin-glass state in (experimentally relevant) finite space dimensions are still subject of controversy. The most prominent of such open questions is the existence of spin-glass ordering in a magnetic field.

The fully-connected mean-field version of the EA model, called the Sherrington-Kirkpatrick (SK) model [2], was solved using the replica method by Parisi [3, 4]; the obtained free energy recently proven to be rigorously exact by Talagrand [5]. In this model, the low-temperature spin-glass phase is characterized by a complex free energy landscape made of many different valleys. This phase also exists for low externally-applied magnetic fields and the so-called de Almeida-Thouless (AT) instability line [6] separates the spin-glass from the paramagnetic phase at finite fields/temperatures. A similar scenario arises in the Bethe lattice approximation (see Fig. 1). However, within the more phenomenological description of spin glasses known as the droplet picture [7] any infinitesimal field destroys the spin-glass order, in stark disagreement with the aforementioned mean-field description. Numerical evidence favoring the absence of a spin-glass state in a field for short-range spin glasses below the upper critical dimension have become stronger [8, 9, 10, 11, 12, 13, 14], although different opinions remain [15, 16, 17, 18].

Capitalizing on the success of studying the susceptibility and the finite-size correlation length [20, 21] to probe the spin-glass phase, we study the problem using a novel numerical approach backed up with analytic calculations on the Bethe lattice. On the numerical side, we use a multi-spin coded version of exchange (parallel tempering) Monte Carlo [22] with a new twist where the replicas “live” in the  $H$ – $T$  plane along a nontrivial path that *guarantees* a crossing with a potential AT line (see

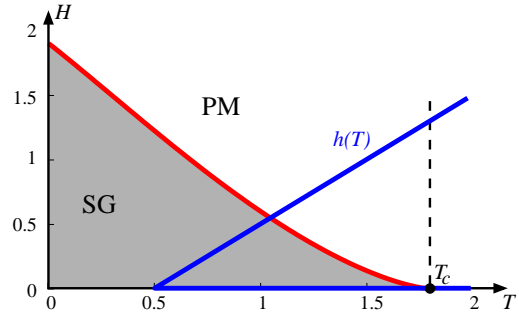


FIG. 1: (Color online) Magnetic field  $H$  versus temperature  $T$  phase diagram of the Ising spin glass on a mean-field random regular graph with connectivity  $c = 6$  with Gaussian interactions computed using the cavity method. The paramagnetic (PM) phase is separated from the spin-glass (SG) phase by the de Almeida-Thouless line (light red curve). The diagonal (dark blue) line  $h(T)$  represents the simulation path followed in the Monte Carlo simulations. Because the path starts at  $T > T_c$  for  $H = 0$  and then increases along a diagonal  $h(T) = r(T - T_{\min})$  in the  $H$ – $T$  plane above  $T_{\min} \ll T_c$  up to a value beyond  $T_c$  (dashed vertical line), an intersection with a putative AT line is guaranteed. The same approach is used for the diluted 3D simulations where  $T_c = 0.663(6)$  [19].

Fig. 1) and that in contrast to Refs. [23, 24] has both ends in the high temperature region where decorrelation is fast. We solve the thermalization problems on diagonal paths found in Ref. [10] by studying the link-diluted version of the model [19] where the cluster moves introduced in Refs. [25] and [19] can be used. In this model, the cluster updates allow the thermalization times to be decreased by a factor of at least  $10^3$ , allowing us to probe relatively large system sizes down to very low temperatures and large magnetic fields. We first demonstrate the efficiency of our strategy by applying it on the model defined on a regular random graph—which corresponds to a Bethe lattice in this context—for which we compute the AT line analytically, generalizing the original result by de Almeida and Thouless for the SK model [6]. The analytical and numerical results for the Bethe lattice agree to high precision. However, results on the 3D model show

no sign of an AT line. The fact that we *do* observe an AT line for the mean-field Bethe lattice, exactly where it is predicted, and *do not* for the short-range 3D Ising spin glass is convincing evidence that the phase diagram is indeed *trivial* and there is no spin-glass state in a field in three dimensions (3D).

*Models* — The spin-glass Hamiltonian is given by

$$\mathcal{H} = - \sum_{i,j} J_{ij} S_i S_j - H \sum_i S_i. \quad (1)$$

The Ising spins  $S_i \in \{\pm 1\}$  have nearest-neighbor interactions. We study the mean-field case where  $N$  spins lie on the vertices of a regular random graph, and the EA model on a cubic lattice of size  $N = L^3$  with periodic boundary conditions, where the interactions  $J_{ij} \in \{-1, 0, 1\}$  are chosen from a link-diluted bimodal distribution with a link occupation probability of 45% [19].

*Theoretical predictions* — Following recent progress in the study of finite-connectivity mean-field systems, it is now possible to study (quite) precisely spin-glass models on Bethe lattices using the cavity method [26]. Within this formalism, first steps in computing the phase diagram in the field-temperature plane have been achieved (see Refs. [27] and [14]). In order to determine the AT line, one needs to compute the onset of divergence of the spin-glass susceptibility  $\chi$  in the paramagnetic phase in which case, thanks to the finite correlation length, the model is equivalent to a spin glass on an infinite tree with random boundary conditions [26] (this is reminiscent of the exact analysis presented in Ref. [28]). We thus consider here the simplest Bethe-Peierls cavity approach for the problem and compute the AT line in this context. We refer the reader to Refs. [26], [27], [14], and [29] for a description of the method. For  $H = 0$ , we recover the well-known result first found by Thouless [30]:  $k[\tanh(\beta_c J)^2]_{\text{av}} = 1$ , where  $\beta_c = 1/T_c$ ,  $k = c - 1$  ( $c$  the connectivity), and  $[\dots]_{\text{av}}$  is a disorder average. For finite external field, one has to perform a numerical solution of the cavity equations to solve the cavity recursion and to compute the point where the susceptibility diverges [29].

Using this approach, we compute points along the AT line for different values of the field  $H$  with Gaussian and bimodal disorder and connectivities  $c = 3$  and 6. We have also checked that the large-connectivity limit of our computation yields the SK result. We find that, close to  $T_c$ , the data scale as  $h_{\text{AT}}(T) \sim (T_c - T)^{3/2}$ —as first predicted in Ref. [30] and checked in Ref. [27]—and the instability line is then approximately linear close to zero temperature [31]. A fit to  $h_{\text{AT}}(T) = a_1(T_c - T)^{3/2} \exp(a_2 T + a_3 T^2)$  gives very accurate results whose precision is within the error of our numerical evaluation of the cavity recursion. For  $c = 6$ , we obtain  $a_1 = 0.786$  (0.875),  $a_2 = 0.111$  (0.221), and  $a_3 = -0.054$  (-0.127) and  $T_c = 1.807$  (2.078) for Gaussian (bimodal) distributed disorder. For  $c = 3$ , we find  $a_1 = 0.785$  (0.827),  $a_2 = 0.251$  (0.413), and  $a_3 = 0.117$  (0.083) and

$T_c = 0.748$  (1.135). The Gaussian case with  $c = 6$  is shown in Fig. 1 (light red curve).

The presence of the instability line in finite-dimensional systems has been criticized before, especially in the context of the droplet model [7]. Other pictures were proposed where no such line is present [32, 33, 34]. It has been also suggested that the line disappears below the upper critical dimension  $d_u = 6$  [12, 35, 36, 37], and even more complex scenarios are possible [38, 39, 40]. We now attempt to clarify this issue in the 3D case.

*Numerical method* — The simulations are performed using exchange Monte Carlo (EMC) [22]. Traditionally, the field is fixed at a constant value and replicas at different temperatures perform a Markov chain in temperature space. There have been alternate approaches where the temperature  $T$  is fixed to  $T < T_c$  and the replicas perform a Markov chain in field space. This method has not proven to be efficient because tunneling across  $H = 0$  requires special moves [23, 24] and especially because in this case no replica has the chance to reach the zero-field high- $T$  phase where relaxation is fast. In order to solve this problem, we propose an EMC method in the  $H$ - $T$  plane (see Fig. 1) at which part of the replicas have labels  $(T, H = 0)$  for temperatures values in the range  $T_{\text{min}} \leq T \leq T_{\text{max}}$  with  $T_{\text{max}} \gg T_c$  (in 3D  $T_{\text{min}} = 0.30$ ). We also couple the replicas in the EMC scheme to a second set of replicas along a diagonal path in the  $H$ - $T$  plane with labels  $(T, H)$  and  $h(T) = r(T - T_{\text{min}})$ ,  $r$  constant. It is important not to choose the slope  $r$  of  $h(T)$  too steep because EMC is least efficient for large fields [23, 24, 41]. In addition,  $T_{\text{max}}(H > 0) > T_c(H = 0)$  has to be chosen to ensure that the a potential AT line is crossed. The method has the advantage to deliver data at zero (horizontal blue path in Fig. 1), as well as finite field (diagonal blue path in Fig. 1). Finally, it is advantageous to choose the slope of the path in the  $H$ - $T$  plane such that it crosses the phase boundary orthogonally (cleaner signal of the transition).

We test equilibration by a logarithmic binning of the data until the data in the last three bins agree within error bars. To access relatively large system sizes in 3D, we use a multi-spin coded version of the program that updates 32 copies of the system in parallel. In order to obtain thermalization in reasonable time, it is necessary to apply the cluster algorithm introduced in Refs. [19] and [25]. The speedup obtained by this approach is of three orders of magnitude over conventional approaches, even for the smallest sizes simulated. Note that the speedup increases with increasing system size; our simulations would not have been possible otherwise. Simulation parameters are listed in Table I.

*Results on the Bethe lattice* — We have computed the connected spin-glass susceptibility using  $\chi = N [\langle q^2 \rangle_T - \langle q \rangle_T^2]_{\text{av}}$  where  $q = 1/N \sum_{i=1}^N q_i$  with  $q_i = S_i^1 S_i^2$  being the overlap at site  $i$  between two independent replicas of the system. Here  $\langle \dots \rangle_T$  represents

TABLE I: Simulation parameters:  $N_{\text{sa}}$  is the number of samples,  $N_{\text{sw}}$  is the number of Monte Carlo sweeps for one sample,  $T_{\text{min}}$  is the lowest temperature simulated,  $H_{\text{max}}$  is the maximum field studied and  $N_r$  is the number of replicas used in the EMC method.  $h_{\text{BL}}(T) = 1.0(T - 0.5)$  for the Bethe lattice (top set); in 3D  $h_{3\text{D}}(T) = 0.7(T - 0.3)$  (bottom set).

$N$	$N_{\text{sa}}$	$N_{\text{sw}}$	$T_{\text{min}}$	$H_{\text{max}}$	$N_r$
64	12834	100000	0.5	2.0	25
128	12689	100000	0.5	2.0	25
256	5107	200000	0.5	2.0	25
512	2546	1000000	0.5	2.0	49
$L$	$N_{\text{sa}}$	$N_{\text{sw}}$	$T_{\text{min}}$	$H_{\text{max}}$	$N_r$
4	20000	200000	0.3	0.49	47
5	20000	400000	0.3	0.49	47
6	20000	400000	0.3	0.49	47
8	10528	1000000	0.3	0.49	51
10	6080	2000000	0.3	0.49	51
12	2944	4000000	0.3	0.49	51

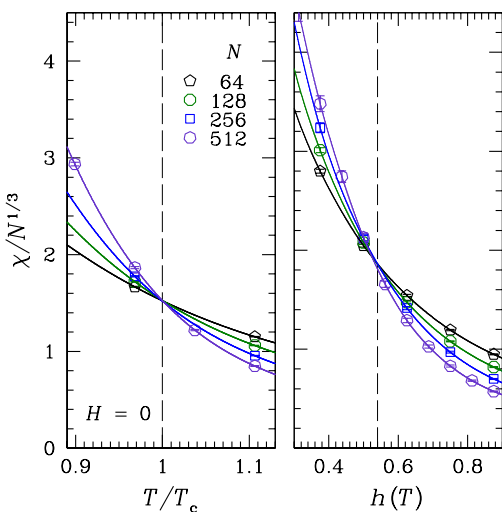


FIG. 2: (Color online) Rescaled susceptibility  $\chi/N^{1/3}$  from Monte Carlo data of the regular random graph model with Gaussian disorder and connectivity  $c = 6$ . Left: Data for zero field cross at the analytically predicted critical temperature  $T_c = 1.807$ . Right: Data along  $h_{\text{BL}}(T) = 1.0(T - 0.5)$ . The crossing point agrees very well with the values in Fig. 1.

a thermal average. The susceptibility of the mean-field model has a finite-size scaling form  $\chi(T, H) = N^{1/3} \tilde{G}(N^{1/3}[T - T_c(H)])$  [23, 24] hence data for different  $N$  should cross at  $T_c$  when plotted as  $\chi/N^{1/3}$  versus  $T$ . This is shown in Fig. 2 for  $c = 6$  and a Gaussian distribution of the interactions: The left panel is at zero field, whereas the right panel is along the diagonal path  $h_{\text{BL}}(T) = 1.0(T - 0.5)$ . In both cases, the data cross in agreement with the analytical results (Fig. 1). Hence our numerical approach allows for a precise detection and location of any putative AT line.

*Results in three dimensions* — In the finite-dimensional system the scaling of the susceptibility re-

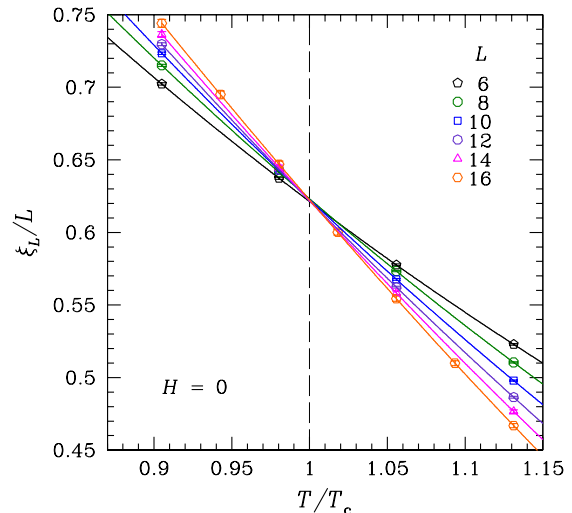


FIG. 3: (Color online) Finite-size correlation length as a function of  $T/T_c$  for the 3D Ising spin glass at zero field with bimodal interactions. The data cleanly cross at  $T_c = 0.663(6)$ .

quires an additional parameter  $\eta$  whose putative in-field value is unknown, as opposed to the mean-field case. We thus prefer to study the transition via the scaling of the finite-size two-point correlation length [20, 21] given by

$$\xi_L = \frac{1}{2 \sin(|\mathbf{k}_{\text{min}}|/2)} \left[ \frac{\chi(0)}{\chi(\mathbf{k}_{\text{min}})} - 1 \right]^{1/2}, \quad (2)$$

where  $\mathbf{k}_{\text{min}} = (2\pi/L, 0, 0)$  is the smallest nonzero wave vector and  $\chi(\mathbf{k})$  the wave-vector-dependent spin-glass susceptibility defined as

$$\chi(\mathbf{k}) = \frac{1}{N} \sum_{i,j} [\langle q_i q_j \rangle_T - \langle q_i \rangle_T \langle q_j \rangle_T]_{\text{av}} e^{i\mathbf{k} \cdot (\mathbf{R}_i - \mathbf{R}_j)}. \quad (3)$$

Note that we used a slightly different definition of the susceptibility than in Ref. [10]. However, the two expressions are equivalent, except that the definition used here requires only two replicas (unlike the four needed in Ref. [10]) thus saving computational resources. The correlation length divided by the system size  $L$  has the scaling relation  $\xi_L/L = \tilde{X}(L^{1/\nu}[T - T_c(H)])$ , where  $\nu$  is the usual critical exponent. When  $T = T_c(H)$  data for different  $L$  cross signaling the existence of a transition.

Data for the 3D model in zero field are shown in Fig. 3. A clear crossing point at  $T_c = 0.663(6)$  is observed, thus signaling the presence of a spin-glass state for system sizes up to  $L = 16$  and in agreement with previous results [19]. In contrast, data along the finite-field branch [ $h_{3\text{D}}(T) = 0.7(T - 0.3)$ ] (see Fig. 1) show no sign of a transition (see Fig. 4). The inset shows a zoom of the data for small fields where the crossing points (arrows) between the different lines wander towards zero for increasing  $L$ . This shows that at temperature  $T = 0.3$ , the instability is below  $h < 0.006$ . This should be compared

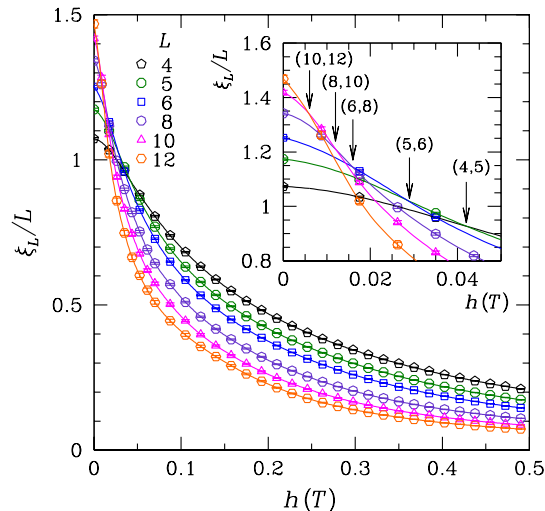


FIG. 4: (Color online) Finite-size correlation length as a function of  $h_{3D}(T) = 0.7(T - 0.3)$  (finite-field branch in Fig. 1) for the 3D Ising spin glass. The apparent crossing of the data wanders towards zero for increasing system size (see inset for a zoom into the low-field region), i.e., there is no sign of a transition for  $H > 0$  (arrows mark crossings between  $L$ -pairs).

with the mean field case where, e.g., for  $c = 3$  with Gaussian couplings (having a similar  $T_c$  as the 3D model), one observes  $h(0.3) \approx 0.26$ , i.e., a value 40 times larger. Performing a one-parameter scaling with fixed volume ratio  $h_c(L) \sim h_c^\infty + b/L^2$  gives  $h_c^\infty = -0.00004(14)$ , i.e., compatible with zero with a  $Q$ -factor of 94.9%. Fixing  $h_c^\infty = 0$  gives  $Q = 99.7\%$ ; i.e., the data suggest the absence of a spin-glass state in a field.

*Summary and discussion* — We have presented calculations of the AT line of a spin glass on a Bethe lattice using the cavity method. These results for the mean-field model on the Bethe lattice allowed the validation of our Monte Carlo simulations where we have observed an AT line close to its predicted value. This is in stark contrast to the 3D Ising spin glass with bimodally-distributed bonds where data for a wide range of fields and temperatures clearly show a lack of ordering in a field.

It would be interesting to study higher-dimensional systems using the method presented here to verify whether or not an AT line is observed above the upper critical dimension [12] and we hope our results will also spark new theoretical developments in this direction.

We thank A. P. Young for helpful discussions. The simulations have been performed on the ETH Zürich Hreidar cluster. H.G.K. acknowledges support from the Swiss National Science Foundation under Grant No. PP002-114713. T.J. acknowledges support from EEC's HPP HPRN-CT-2002-00307 (DYGLAGEMEM) and FP6 IST contracts under IST-034952 (GENNETEC).

- [2] D. Sherrington and S. Kirkpatrick, Phys. Rev. Lett. **35**, 1792 (1975).
- [3] M. Mézard, G. Parisi, and M. A. Virasoro, *Spin Glass Theory and Beyond* (World Scientific, Singapore, 1987).
- [4] A. P. Young, ed., *Spin Glasses and Random Fields* (World Scientific, Singapore, 1998).
- [5] M. Talagrand, Ann. of Math. **163**, 221 (2006).
- [6] J. R. L. de Almeida and D. J. Thouless, J. Phys. A **11**, 983 (1978).
- [7] D. S. Fisher and D. A. Huse, Phys. Rev. Lett. **56**, 1601 (1986).
- [8] G. Migliorini and A. N. Berker, Phys. Rev. B **57**, 426 (1998).
- [9] J. Houdayer and O. C. Martin, Phys. Rev. Lett. **82**, 4934 (1999).
- [10] A. P. Young and H. G. Katzgraber, Phys. Rev. Lett. **93**, 207203 (2004).
- [11] P. E. Jönsson *et al.*, Phys. Rev. B **71**, 180412(R) (2005).
- [12] H. G. Katzgraber and A. P. Young, Phys. Rev. B **72**, 184416 (2005).
- [13] M. Sasaki *et al.*, Phys. Rev. Lett. **99**, 137202 (2007).
- [14] F. Krzakala, Prog. Theor. Phys. Supp **157**, 77 (2005).
- [15] J. C. Ciria *et al.*, J. Phys. A **26**, 6731 (1993).
- [16] E. Marinari *et al.*, J. Phys. A **31**, 6355 (1998).
- [17] F. Krzakala *et al.*, Phys. Rev. Lett. **87**, 197204 (2001).
- [18] G. Parisi (2007), (arXiv:cond-mat/0711.0369).
- [19] T. Jörg, Phys. Rev. B **73**, 224431 (2006).
- [20] M. Palassini and S. Caracciolo, Phys. Rev. Lett. **82**, 5128 (1999).
- [21] H. G. Ballesteros *et al.*, Phys. Rev. B **62**, 14237 (2000).
- [22] K. Hukushima and K. Nemoto, J. Phys. Soc. Jpn. **65**, 1604 (1996).
- [23] A. Billoire and B. Coluzzi, Phys. Rev. E **67**, 036108 (2003).
- [24] A. Billoire and B. Coluzzi, Phys. Rev. E **68**, 026131 (2003).
- [25] T. Jörg, Prog. Theor. Phys. Supp. **157**, 349 (2005).
- [26] M. Mézard and G. Parisi, Eur. Phys. J. B **20**, 217 (2001).
- [27] A. Pagnani *et al.*, Phys. Rev. E **68**, 046706 (2003).
- [28] J. M. Carlson *et al.*, Europhys. Lett. **5**, 355 (1988).
- [29] O. C. Martin *et al.*, J. Stat. Mech. P09006 (2005).
- [30] D. J. Thouless, Phys. Rev. Lett. **56**, 1082 (1986).
- [31] Our results contradict the results of Ref. [27] because there too small systems were used. Our results are recovered for larger system sizes.
- [32] F. Krzakala and O. C. Martin, Phys. Rev. Lett. **85**, 3013 (2000).
- [33] M. Palassini and A. P. Young, Phys. Rev. Lett. **85**, 3017 (2000).
- [34] C. M. Newman and D. L. Stein, J. Phys.: Condensed Matter **15**, 1319 (2003).
- [35] A. J. Bray and S. A. Roberts, J. Phys. C **13**, 5405 (1980).
- [36] T. Temesvári *et al.*, Euro. Phys. J. B **25**, 361 (2002).
- [37] I. R. Pimentel *et al.*, Phys. Rev. B **65**, 224420 (2002).
- [38] T. Temesvári and C. de Dominicis, Phys. Rev. Lett. **89**, 097204 (2002).
- [39] T. Temesvári, J. Phys. A **39**, L61 (2006).
- [40] T. Temesvári, Nucl. Phys. B **772**, 340 (2007).
- [41] J. J. Moreno *et al.*, Int. J. Mod. Phys. C **14**, 285 (2003).

[1] S. F. Edwards and P. W. Anderson, J. Phys. F: Met. Phys. **5**, 965 (1975).